J. Membrane Biol. 47, 129–143 (1979)

The Effective Configuration of a Molecule in Ultrafiltration: Its Definition and Determination

E. Middleton

Department of Hormone Physiology, Imperial Cancer Research Fund, Lincoln's Inn Fields, London, WC2A3PX

Received 26 June 1978; revised 1 February 1979

Summary. The time taken to descend through a measured depth of glycerol was recorded for some metal boxes, cylinders, ellipsoids and spheres having axial ratios from 0.2 to 2.4. The results were used to determine the relation between each nonspherical form, its axial ratio, and the radius of its dynamically equivalent sphere with respect to glycerol. Expressed in dimensionless terms, these relations closely predict the *real* gross configuration of four regularly shaped molecules (inulin, ribonuclease, hemoglobin and hen egg-white lysozyme), and sensibly predict the *effective* gross configuration of one irregularly shaped molecule (γGl immunoglobulin) from their known axial ratios and Stokes-Einstein radii. Similarly, they predict the *effective* gross configuration of a molecule whose real shape is not known (serum albumin). Since the relations established for the models apply to all the molecules considered, it seems likely that they can be used in conjunction with membrane-diffusion studies (E. Middleton, 1975, *J. Membrane Biol.* **20**:347) and free-diffusion studies to determine the effective configuration in ultrafiltration of any molecule.

The effective configuration of a molecule characterizes its behavior in a particular situation and has been unequivocally defined for free diffusion (i.e., the Stokes-Einstein sphere) and for sedimentation (i.e., the Perrin ellipsoid), but, to our knowledge, not for filtration. It is important to note that in free diffusion and sedimentation the effective configuration generally, though not invariably, differs from the real gross configuration in terms of shape and axial dimensions and is therefore imaginary.

In contrast, the effective configuration of a molecule in filtration, though also generally imaginary in shape, must invariably have *real* dimensions for its major and median axes, since these respectively determine when filtration begins to be restricted and finally ceases (Middleton, 1975, 1977). To satisfy the diffusion component of filtration (Chang *et al.*, 1975), the effective configuration must also have the *hydrodynamically* determined Stokes-Einstein radius of the molecule it represents (Nozaki *et al.*, 1976).

0022-2631/79/0047-0129 $03.00

These requirements make it impossible to represent unequivocally all molecules in all filtration situations by a single shape, though effective representation might be achieved by using a small selected group of shapes. The most likely group would seem to be the box, cylinder, and ellipsoid, since these might adequately represent highly angular, moderately angular and slightly angular molecules, respectively. Interpolation between these shapes would provide an infinity of other regular shapes.

It would be useful if the relation between the effective configuration in filtration, the effective configuration in diffusion (i.e., the Stokes-Einstein sphere), and the real axial ratio of a molecule could be established for each of these three basic shapes. No theoretical or practical study of any such relation seems to have been made to date, presumably because the kinetics are formidable, and few *sets* of Stokes-Einstein radii and of real axial dimensions are available.

The present paper establishes *numerical* (nontheoretical) relations between the axial ratios of large-scale models of the proposed basic shapes and the radii of their respective equivalent spheres with respect to motion in a viscous fluid, and examines whether these relations apply at the molecular level by using as examples those molecules for which the requisite data are available.

Materials and Methods

The 44 models described here, and shown from two orthogonal directions in Fig. 1, were machined from aluminium alloy ($\rho = 2.687$) and had nearly identical weights (2.973 ± 0.015 g, mean $\pm$ SEM). Three main sets consisted of boxes, cylinders, and ellipsoids, and covered a range of axial ratios (L/R = semi-length/radius) from about 0.2 (oblate form) to 2.4 (prolate form). Two subsidiary sets were intended to cover forms intermediate between the sphere and the symmetrical cylinder (cylindrical ellipsoids; $g_1 - g_4$, Fig. 1) and between this latter shape and the symmetrical box (cylindrical boxes; $f_a - f_c$, Fig. 1). The remaining model was a cylinder machined to represent the proportions and internal configuration of the inulin molecule (Middleton, 1977).

The studies also included two duralumin balls (radii (S) = 0.4760, 0.7145 cm; $\rho = 2.782$), three steel balls ($S = 0.3820$, 0.4595, 0.6125 cm; $\rho = 7.418$), and three phosphor-bronze balls ($S = 0.4595$, 0.5340, 0.6125 cm; $\rho = 8.736$).

Preliminary experiments showed that the models assumed positions of maximum drag (*cf.* Boucher, 1973) when allowed to fall freely through glycerol – in other words, the prolate bodies ($L > R$) could not descend end-on, or the oblate bodies ($L < R$) edge-on. It was required however, that both forms descend in their unnatural as well as natural positions, since it seemed reasonable to assume that the mean time of descent in both positions equals the time of descent of a randomly tumbling body. To achieve unnatural descent, the center of gravity of some of the bodies was shifted from one end (prolate), or one side (oblate) of the body by drilling an appropriate hole and plugging it with

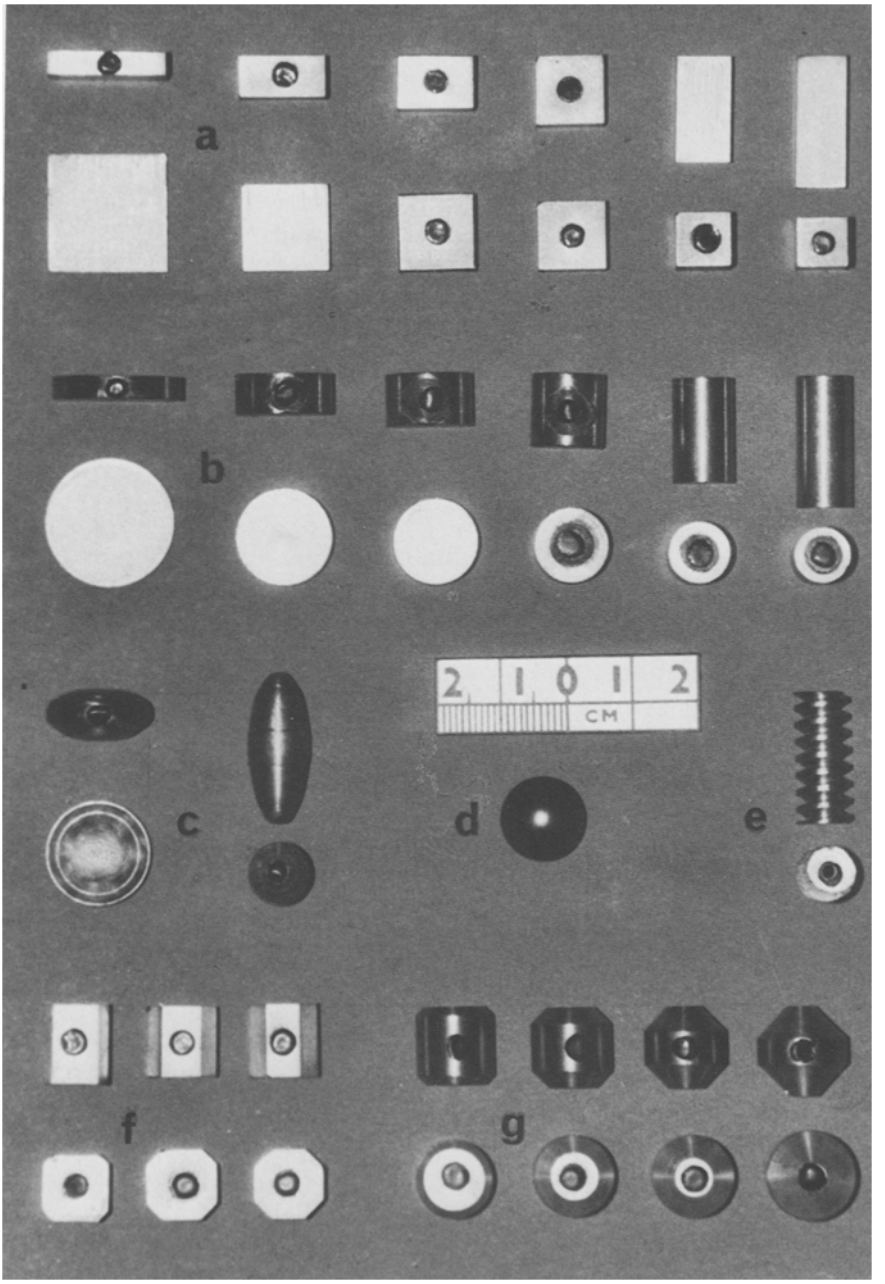

Fig. 1. Paired orthogonal views of the 22 aluminium models used in the studies (44 models in all). The 32 models containing lead inserts (*see* text) are easily recognized. (*a*): boxes; (*b*): cylinders; (*c*): ellipsoids; (*d*): a sphere having volume approximately equal to that of the models; (*e*): cylinders modified to represent the inulin molecule (*see* text); (*f*): "cylindrical boxes"; (*g*): "cylindrical ellipsoids". The individual members of groups *f* and *g* are referred to in text as $f_a - f_c$ and $g_1 - g_4$ (left to right). Scale as shown

a weight of lead equal to that of the lost alloy. The modified bodies are identified in Fig. 1.

It is as well to note here that the motion of a body (as opposed to a molecule) tumbling randomly through a fluid has not been analyzed to date, presumably because such motion does not normally occur. This leads to one other assumption when considering "wall" effects between the models and the containing vessel (*see Results*).

The time of descent through the central 45 cm of a 69-cm column of glycerol ($\rho = 1.266$) was recorded for each of the 52 bodies. The container—a glass cylinder having a diameter of 9.5 cms—was then emptied, the bodies were retrieved, and the container was refilled with the same glycerol. The glycerol was allowed to equilibrate for 45 min after which a further trial was made. There were nine trials in all, each taking 15 min to complete and comprising all bodies. The temperature of the glycerol remained constant at 20.8 °C throughout the span of the experiments (8 hr). The densities quoted in this section were determined, not assumed.

Results

The coefficients of variation (SD × 100/mean) of the results increased with increasing angularity of the bodies: they ranged from 6.8% for the spheres to 9.6% for the cylinder machined to represent the inulin molecule. Most of this variation was due to the descent times decreasing slightly as the trials proceeded, but since the overall rate of decrease was small (-0.067 ± 0.004 sec/hr (mean ± SEM) in the context of each trial period (15 min), this experimental drift can be safely ignored in the calculations which follow.

Spheres

The raw data from the spheres was used in conjunction with Stoke's law ($\eta = 2gS^2(\rho_S - \rho_G)/9v$) to determine the viscosity of the glycerol used in these studies, and thence to assess whether the experimental procedures were sound or not. Clearly they were, since the relation between the apparent viscosity (η_S) and the radius squared (S^2) proved to be reasonably linear ($\eta_S = 10.42(S^2) + 11.48$; $r = 0.944$), and the intercept ($\eta_0 = 11.48$) was in the viscosity range 11.1–13.8 P given by Kaye and Laby (1973) for glycerol of purity 99–100% and temperature 20.8 °C.

The slope of the line (10.42 P/cm^2) indicates that the fluid flux density between the cylinder and the spheres increased greatly as the size of the spheres increased. For an asymmetrical body, this "wall" effect will be relatively large or small depending on whether the body sediments in a position of maximum or minimum drag. Since the semi-axial lengths

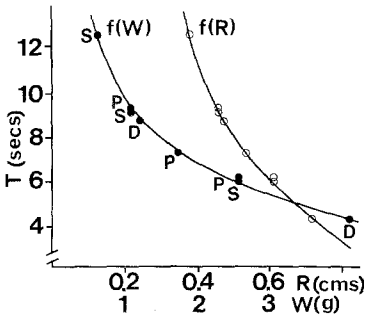

Fig. 2. The time of descent of 8 balls as a function of their radius (R) and of their weight (W). The times and weights are adjusted as if all the balls had a density of 2.687 (*see* text). *P:* phosphor-bronze; *S:* steel; *D:* duralumin

of a body encompass, or nearly equal, the radius of its equivalent sphere, it seems likely that the mean "wall" effect of a randomly tumbling body will be substantially the same as that of its equivalent sphere. In the absence of any evidence to the contrary, we shall assume this to be so when comparing models and spheres.

With these comparisons in mind, the descent times of the spheres are plotted in Fig. 2 in terms of their weights (W) and radii (S), as if all the spheres were of the same material as the models. This involved using the relation $T_A/T_M=(\rho_M-\rho_G)/(\rho_A-\rho_G)$, where T=time of descent; ρ=density; A=aluminium alloy; M=duralumin, steel, or phosphor-bronze; and G=glycerol. The recalculated results present two well-defined curves whose "least mean squares" quadratic equations are, respectively, $T=14.8067-5.3915\ W+0.7152\ W^2$ and (in reverse form to its figure) $S=1.0961-0.1011\ T+0.0035\ T^2$.

Main Models

The equation $T=f(W)$ was used to calculate the time of descent of each main and each subsidiary model as if it had the mean weight of all these models (2.973 g). For all practical purposes, changing the size but not the shape of a body has relatively the same effect on descent time for all shapes so long as the viscosity of the milieu fluid is greater than about 7.2 P (Pettyjohn & Christiansen, 1948), so that $T=f(W)$ for the spheres applies equally well for the models so long as the equation constant (14.8067) is changed to satisfy the particular values for T and W.

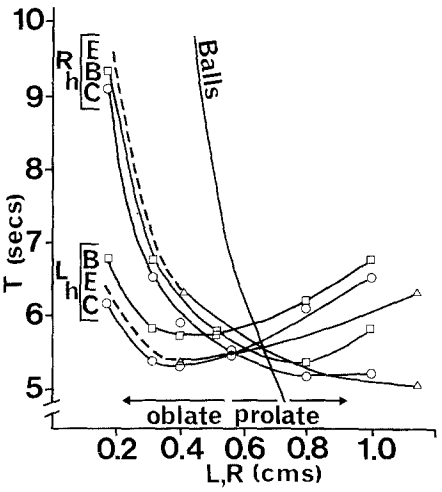

Fig. 3. The descent time as a function of the semi-length (L) for the main models, and of the radius (R) for the spheres. R_h: descent with the radius horizontal; L_h: descent with the semi-length horizontal. △: ellipsoids; ○: cylinders; □: boxes

The weight-normalized descent times for the boxes, cylinders, and ellipsoids are plotted in Fig. 3 where they can be compared with the density-normalized descent times for the spheres. There are two intersecting curves for each set of models, one representing the models falling with their lengths horizontal, the other with them vertical. The upper and lower arms of each pair of curves respectively represent descent in the natural and unnatural positions, while their intersection represents descent in which there is no preferred position.

The equivalent radius ($\hat{S}$) of a randomly tumbling body is presumably the mean of the equivalent radii in both descent positions, and these values are calculated from the equation $S=f(T)$ given above. The mean of these values is plotted in Fig. 4 where it can be compared with the semi-axes of the model. $\hat{S}$ was invariably intermediate between L and R for the ellipsoids, and mostly so for the cylinders and boxes; for these latter shapes, however, $\hat{S}$ was slightly larger than L or R for values of L/R in the range 0.7–1.3. For each of the main models (except the symmetrical cylinder) $\hat{S}$ was smaller than the radius of the sphere of equal volume (0.642 cm).

Subsidiary Models

The "cylindrical boxes" (f_a-f_c, Fig. 1 left to right) had equivalent radii of 0.664, 0.652, and 0.633 cm, respectively, and the "cylindrical

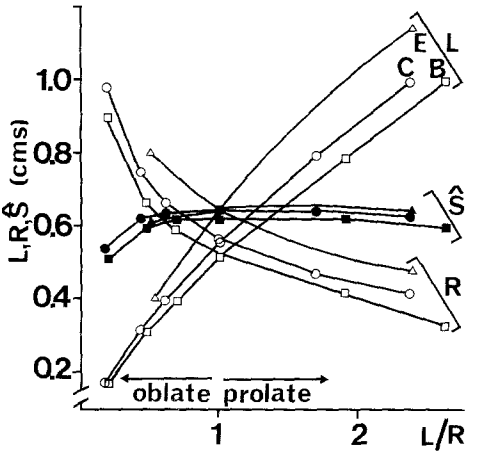

Fig. 4. The semi-length (L), radius (R), and the equivalent hydrodynamic radius ($\hat{S}$) of the main models as a function of their axial ratio (L/R). Open symbols: primary dimensions (L, R); closed symbols: derived dimensions ($\hat{S}$). △▲: ellipsoids; ○●: cylinders; □■: boxes

ellipsoids" (g_1-g_4, Fig. 1, left to right) radii of 0.647, 0.652, 0.694, and 0.660 cm, respectively. In contrast to the main models, all these values except one were greater than the radius of the sphere of equal volume (0.642 cm). The "cylindrical ellipsoids" were strictly comparable with each other, since they all had an axial ratio equal to 1; we note that $\hat{S}$ first increased, and then decreased, as the models became less cylindrical. No comment is possible about the "cylindrical boxes" in this respect, since one of the three models was designed incorrectly, being prolate in shape though of correct volume.

The natural and unnatural descent times of the cylinder machined to represent the inulin molecule were considerably greater than those of the equivalent unmodified cylinder (9.00 and 7.27 sec, respectively, against 6.65 and 5.23 sec) and consequently $\hat{S}$ for the modified cylinder was smaller than for the unmodified cylinder (0.507 against 0.632 cm). However, when $\hat{S}$ was recalculated for the modified cylinder using descent times for the spheres having a density which took account of the glycerol within its thread (alloy+glycerol: 2.285; alloy alone: 2.687), it was then found to be roughly the same as for the unmodified cylinder (0.635 against 0.632 cm). The relation between L, R and $\hat{S}$ (0.966:0.418:0.635 cm=2.31:1.00:1.52) was nearly the same as for the inulin molecule (25:10.5:15.2 Å=2.38:1.00:1.45; Middleton, 1975, 1977).

Discussion

The relation between the motion of randomly tumbling bodies down a cylindrically-confined fluid, and that of molecules filtering through a membrane is unclear. The former has not been analyzed at all, and the latter only for spherical molecules. This does not invalidate the present studies, since all that is required for equivalence between the gross configuration of a molecule and the actual configuration of a model is that the same *numerical* relation between L, R and $\hat{S}$ holds for both.

Perhaps we should note that Scheidegger (1963), in a comprehensive survey of hydromechanics in porous media, finds that the subject stands essentially on a heuristic basis, and will continue to do so until the appropriate *statistical* techniques are developed to deal with the problems involved. To our knowledge, the situation has not changed.

Models

Because we wish to discuss the models in terms of molecules, and without recourse to theory, the results must be expressed in a dimensionless and empirical form. In the event, we have expressed the axial ratio (L/R) in terms of $(\hat{S}/R)$, and Fig. 5 shows this relation for boxes, cylinders and ellipsoids. The following "least mean squares" equations fit the curves over the range studied perfectly $(r=1.0000)$:

Ellipsoids $(Y=L/R;\ X=\hat{S}/R)$

$$Y=-4.1450+24.2164\,X-50.4516\,X^2+42.8649\,X^3-2.2924\,X^4 -15.1091\,X^5+5.9169X^6$$

Cylinders

$$Y=-6.7574+32.7305\,X-53.4960\,X^2+27.3183\,X^3+15.9993\,X^4 -20.9906\,X^5+5.8528\,X^6$$

Boxes

$$Y=-11.9898+56.1413\,X-91.6399\,X^2+54.2204\,X^3+9.6231\,X^4 -22.0539\,X^5+6.2815\,X^6$$

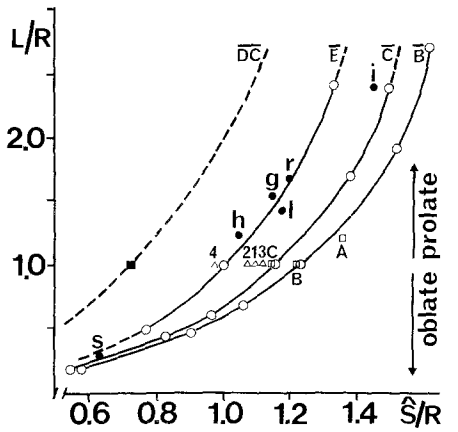

Fig. 5. The axial ratio of a body (L/R) as a function of the ratio between its equivalent and real radii ($\hat{S}/R$). $\bar{E}$: ellipsoids; $\bar{C}$: cylinders; $\bar{B}$: boxes; $\bar{D}\bar{C}$: double-cones. ○: main models; △: cylindrical ellipsoids (*g*, Fig. 1); □: cylindrical boxes (*f*, Fig. 1). ■: estimated point for the symmetrical double-cone and its provisional curve. ●: molecules; inulin (*i*), ribonuclease (*r*), γGl immunoglobulin (*g*), hen egg-white lysozyme (*l*), hemoglobin (*h*), serum albumin (*s*). *See* text for reference sources

The results for the subsidiary models are shown in Fig. 5 where they can be compared with the curves for the main models. The "cylindrical ellipsoids" do not locate in the order expected (*compare* Figs. 1 and 5), and the least cylindrical member of this group (g_4, Fig. 1) locates well to the left of the curve for ellipsoids, rather than to the right. To a lesser extent, this apparent disorder applies to the "cylindrical boxes" as well.

Where the least cylindrical of the "cylindrical ellipsoids" is concerned, its location in Fig. 5, and its shape (g_4, Fig. 1) suggests that it lies directly between the sphere and a model consisting of two equal cones base-to-base. Calculations show that the semi-axes and equivalent radius of this model would be precisely 0.808 and about 0.582 cm, respectively, and its location in Fig. 5, $Y=1.00$, $X=0.72$. This model would be the central member of a set of double-cones whose provisional curve is shown in Fig. 5.

The free-settling rates of some other shapes (isometric cube-octahedrons, octahedrons, cubes, tetrahedrons, and spheres) have been studied by Pettyjohn and Christiansen (1948), but it is impossible to deduce Fig. 5-type curves from their results, since the bodies descended in positions of maximum drag. Their results do indicate, however, that the curve for tetrahedrons probably lies well to the right of the curves

shown in Fig. 5, so that the one prolate "cylindrical box" (f_a, Fig. 1) in the present studies probably lies between the box and the tetrahedron rather than between the box and the cylinder as was intended.

Attempts to explain the seemingly anomalous locations of the subsidiary models in terms of their dimensions and shapes proved unsuccessful, emphasizing just how difficult it is to quantify the opposing effects of cutting edges and piercing points on the one hand, and of dragging surfaces on the other. It seems likely that the locations of the subsidiary models indicate their effective configurations in terms of the main models rather than their real shapes. In other words, effective configurations along the direct path between the symmetrical cylinder and the sphere (for example) would converge to the spherical shape in a smoother fashion than do the "cylindrical ellipsoids" ($g_1 - g_4$, Fig. 1). Presumably, effective configurations between the curves for the main models could be predicted from the equations using "critical path" techniques, but this is beyond the scope of the present paper.

Molecules

At the start of these studies we were not too hopeful of their relevance to the molecular situation, since sedimentation rates are *directly* proportional to mass, whereas diffusion rates are *inversely* proportional to mass. Off-setting this difference, however, is the fact that oblate bodies (for example) appear to have large mass when sedimenting edge-on and small mass when sedimenting face-on, whereas oblate molecules appear to have small mass when diffusing edge-on and large mass when diffusing face-on. It follows that the average effective radius of a randomly tumbling body may well represent that of a diffusing molecule.

Since the structure of a macromolecule in solution can differ noticeably from its (dry) crystalline structure (Timchenko *et al.*, 1978) and its level of hydration is generally uncertain (Hagler & Moult, 1978), values for L, R and $\hat{S}$ must be determined *hydrodynamically* if we are to assess whether the relationships between L/R and $\hat{S}/R$ established for the models do apply at the molecular level. Thus, the "ultrafiltration" axes of the solvated molecule should be determined by membrane-diffusion methods (Middleton, 1975), and its Stokes-Einstein radius by measuring its coefficient of diffusion in free solution (Edsall, 1953; Nozaki *et al.*, 1976).

Unfortunately, we must use molecules whose molecular dimensions have been determined by X-ray diffraction methods, otherwise we are

restricted to just one example (inulin). Even so, there are surprisingly few molecules for which both molecular (as distinct from unit crystal) dimensions *and* $\hat{S}$ are known, and the complete list would seem to be: ribonuclease (Carlisle *et al.*, 1974); hemoglobin (Muirhead & Perutz, 1963); γGl immunoglobulin (Sarma *et al.*, 1971); and hen egg-white lysozyme (Blake *et al.*, 1965). The Stokes-Einstein radii of these molecules can be determined from their coefficients of diffusion as listed by Smith (1970), and for inulin as listed by Bunim, Smith and Smith (1937) and Phelps (1965).

In calculating L/R and $\hat{S}/R$ for the proteins, we have added 2.5 Å to each of their "X-ray diffraction" dimensions on the assumption that surface solvation is limited to a monolayer of water molecules. No great error arises if the level of solvation is slightly greater than this, since these molecules are fairly large compared with the water molecule. The value for $\hat{S}$ remains unchanged, since it unequivocally refers to the solvated molecule. Associated values for L/R and $\hat{S}/R$ are plotted in Fig. 5 for inulin and for each of the four protein molecules; their locations here indicate their effective configurations. These configurations are drawn in Fig. 6 where they can be compared with their respective Stokes-Einstein spheres and real configurations.

It seems fairly clear from these varied examples that the relations established for the models do in fact apply at the molecular level. This finding is not so strange as might first appear, since the studies of Pettyjohn and Christiansen (1948) indicate that the ratio $\hat{S}/R$ in free-settling experiments depends on the viscosity of the milieu fluid, so that such experiments might be made to simulate free diffusion by a suitable choice of viscosity. Fig. 7 shows that our results for the cube and those of Pettyjohn and Christiansen (1948) are substantially the same where the relation between $\hat{S}/R$ and viscosity is concerned, and we note that if the chosen viscosity (11.47 P) had been lower than was actually the case, the present studies would have failed to simulated molecular diffusion.

The results of these studies suggest that the way in which $\hat{S}$ changes with alteration in configuration is not as generally supposed for molecules. Lieb and Stein (1971) state that if the transport milieu is water—in other words, if the diffusant molecule is considerably larger than the milieu molecule—any departure from the spherical shape by the diffusant molecule results in an increase in its Stokes-Einstein radius. The present studies indicate however, that while this may be generally true for changes which maintain axial equality ($L = R$), it is not true otherwise. The equiva-

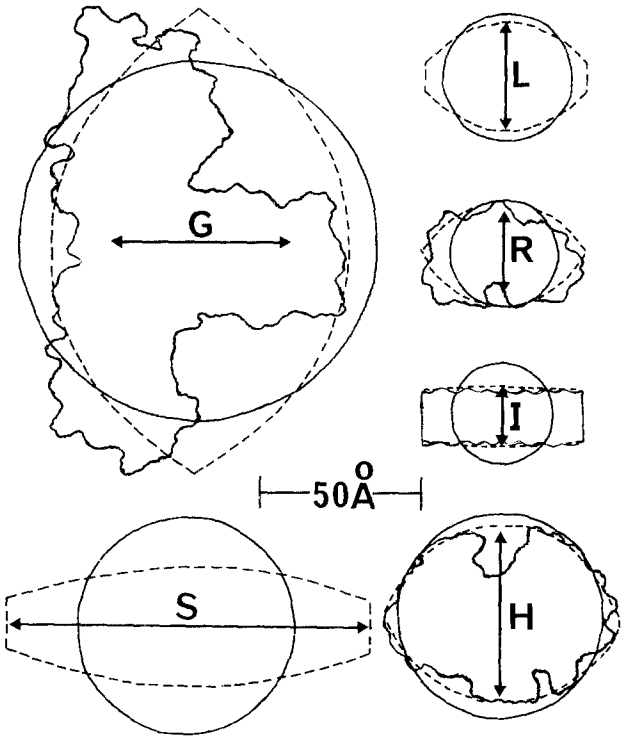

Fig. 6. A comparison of the effective configuration of a molecule in ultrafiltration (broken line), its Stokes-Einstein sphere in free-diffusion, and (where known) its real configuration. Scale as shown; arrows represent axial lengths orthogonal to the paper. *G:* γGl immunoglobulin; *S:* serum albumin; *L:* hen egg-white lysozyme (real and effective configurations nearly identical); *R:* ribonuclease; *I:* inulin; *H:* haemoglobin. Reference sources given in text

lent radius was certainly greater than that of the sphere of equal volume for six of the eight symmetrical models, but for twelve of the thirteen asymmetrical models it was smaller. Presumably, increased asymmetry aids movement of molecules through fluids, whereas increased angularity hinders it.

Even the situation where $L/R = \hat{S}/R = 1$ is not as simple as might first appear since, although the Stokes-Einstein sphere is now the effective configuration in ultrafiltration as well as in free diffusion, its volume will be equal to or greater than that of the real configuration, depending on whether the latter is spherical or not. For example, interpolation between the "cylindrical ellipsoids" suggests that the member located at $L/R = \hat{S}/R = 1$ has an effective radius of 0.664 cm, which is greater than the radius of the sphere of equal volume (0.642 cm).

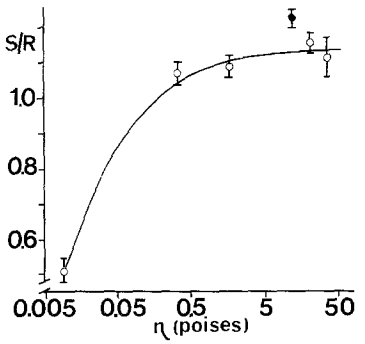

Fig. 7. The ratio between the dynamically equivalent radius and real radius of a cube as a function of the viscosity of the milieu fluid. ●: present studies; ○: studies of Pettyjohn *et al.* (1948). The standard errors refer to nine or twelve sizes of cube in the latter studies, and to one size in the present studies

The results of the cylinder modified to represent the inulin molecule are of particular interest, since they indicate that the real shape, the Stokes-Einstein shape in free-diffusion, and the effective shape in ultrafiltration, all have the same density, and that this parameter includes a contribution by the fluid within the molecular matrix.

Practical Considerations

The axial ratio of a body is defined here as the ratio of its semi-length (L) and radius (R), this ratio being greater or smaller than unity depending on whether the body is prolate or oblate. The axial ratio of a molecule is defined in exactly the same way, though Yang (1961) refers to an oblate molecule (serum albumin) having an axial ratio of 3.5. This value presumably represents the ratio of the molecule's major and median axes, and is therefore the reciprocal of the true axial ratio.

Strictly speaking, of course, if the molecules and membrane pores are precisely and respectively rectilinear and circular, a different interpretation of "ultrafiltration" measurements would be needed, for in this unlikely situation the measured axes would not invariably be the axes of the present models. For instance, when the results for the boxes are recalculated in terms of their appropriate diagonals, their effective configurations appear to be "ellipsoidal double-cones" aligned along the major internal diagonals of the boxes.

Our definitions of effective configuration are based on models having three semi-axes (L, R_1 and R_2) mutually orthogonal, and two of these semi-axes (R_1 and R_2) equal. Since axial equality is not a usual property of molecules, we should note that an effective configuration having $R_1 =$

R_2 can represent a real configuration having $R_1 > R_2$ simply by off-setting the larger volume about its girth by a smaller volume about its shoulders (*cf.* γ-globulin, Fig. 6). This arises from the fact that $\hat{S}$, and therefore $\hat{S}/R$, decreases as R_2 decreases, with the result that, for a given L/R_1, the effective configuration becomes increasingly ellipsoidal or double-coned, depending on whether it lies to the right or left of the curve for ellipsoids. In the latter case, the effective configuration may even locate to the left of the provisional curve for double-cones, for this area represents double-cones having $R_1 > R_2$.

It is inherently difficult to distinguish between prolate and oblate molecules from membrane-diffusion studies, since these yield L and R_1 for prolate molecules and R_1 and R_2 for oblate molecules. In this uncertain situation, the asymmetry of the Fig. 5 curves with respect to their axes can be used to decide between the two shapes, since only correct naming of the paired determinations will result in a sensible fit between the plotted point and the curves.

Serum albumin is an important example here, since, from X-ray diffraction studies alone, Low (1952) concludes that the molecule is prolate, whereas Yang (1961) concludes that it is oblate. The present studies clearly indicate an oblate molecule, for the ratio of its Stokes-Einstein radius (34.5 Å; Smith, 1970) to its cut-off pore radius (55 Å; Jacobs, 1974) is far too small (0.62) for the molecule to be prolate. A provisional effective oblate model for the serum albumin molecule, based on an axial ratio, in present terms, of 0.29 (Yang, 1961) is shown in Figs. 5 and 6.

The present studies are also relevant to the estimation of membrane permeability based on the major and median semi-axes of a solvated marker molecule. In biological systems, this estimation is best made by using two molecules of different size, since their relative passage through a membrane is less dependent on the mode of transport than is their separate passage (Middleton, 1975).

In conclusion, we would hope that these simple studies may provide a more practical approach to the twin subjects of membrane permeability and effective molecular configuration than is currently the case.

We would like to thank Mr. G.R. Glayzer for machining the models and Mr. A.D. Leach for photographing them. Also Dr. L. Martin for encouraging and criticizing the studies.

References

Blake, C.C.F., Koenig, D.F., Mair, G.A., North, A.C.T., Phillips, D.C., Sarma, V.R. 1965. Structure of hen egg-white lysozyme. A three-dimensional Fourier synthesis at 2 Å resolution. *Nature (London)* **206**:757

Boucher, D.F. 1973. Particle dynamics. *In:* Chemical Engineers' Handbook. R.H. Perry and C.H. Chilton, editors. pp. 5–62. Mcgraw-Hill, New York–London

Bunim, J.J., Smith, W.W., Smith, H.W. 1937. The diffusion coefficient of inulin and other substances of interest in renal physiology. *J. Biol. Chem.* **118**:667

Carlisle, C.H., Palmer, R.A., Mazumdar, S.K., Gorinsky, B.A., Yeates, D.G.R. 1974. The structure of ribonuclease at 2.5 Angstrom resolution. *J. Mol. Biol.* **85**:1

Chang, R.L.S., Robertson, C.R., Deen, W.M., Brenner, B.M. 1975. Permselectivity of the glomerular wall to macromolecules. 1. Theoretical considerations. *Biophys. J.* **15**:861

Edsall, J.T. 1953. The size, shape and hydration of protein molecules. *In:* The Proteins. H. Neurath and K. Bailey, editors. Vol. 1, Part B, p. 628. Academic Press, New York

Hagler, A.T., Moult, J. 1978. Computor simulation of the solvent structure around biological macromolecules. *Nature (London)* **272**:222

Jacobs, S. 1974. Ultrafilter membranes in biochemistry. *In:* Methods of Biochemical Analysis. D. Glick, editor. p. 330. John Wiley & Sons, New York–London–Sydney–Toronto

Kaye, G.W.C., Laby, T.H. 1973. Tables of Physical and Chemical Constants. Longman, London

Lieb, W.R., Stein, W.D. 1971. The molecular basis of simple diffusion within biological membranes. *In:* Current topics in Membranes and Transport. F. Bronner and A. Kleinzeller, editors. p. 1. Academic Press, New York–London

Low, B.W. 1952. Preparation and properties of serum and plasma proteins. XXXIV. An X-ray study of crystalline human serum albumin preparations. *J. Am. Chem. Soc.* **74**:4830

Middleton, E. 1975. Passage of inulin and *p*-aminohippuric acid through artificial membranes: Implications for measurement of renal function. *J. Membrane Biol.* **20**:347

Middleton, E. 1977. The molecular configuration of inulin: Implications for ultrafiltration theory and glomerular permeability. *J. Membrane Biol.* **34**:93

Muirhead, H., Perutz, M.F. 1963. Structure of haemoglobin. A three-dimensional Fourier synthesis of reduced human haemoglobin at 5.5 Å resolution. *Nature (London)* **199**:633

Nozaki, Y., Schechter, N.M., Reynolds, J.A., Tanford, C. 1976. Use of gel chromatography for the determination of the Stokes radii of proteins in the presence and absence of detergents. A reexamination. *Biochemistry* **15**:3884

Pettyjohn, E.S., Christiansen, E.B. 1948. Effect of particle shape on free-settling rates of isometric particles. *Chem. Eng. Prog.* **44**:157

Phelps, C.F. 1965. The physical properties of inulin solutions. *Biochem. J.* **95**:41

Sarma, V.R., Silverton, E.W., Davies, D.R., Terry, W.T. 1971. The three-dimensional structure at 6 Å resolution of a γGl immunoglobulin molecule. *J. Biol. Chem.* **246**:3735

Scheidegger, A.E. 1963. Hydrodynamics in porous media. *In:* Encyclopedia of Physics. S. Flugge, editor. Vol. VIII/2, Fluid Dynamics II, p. 625. Springer-Verlag, Berlin–Göttingen–Heidelberg

Smith, M.H. 1970. Molecular weights of proteins and some other materials including sedimentation diffusion and frictional coefficients and partial specific volumes. *In:* Handbook of Biochemistry and selected data for Molecular Biology. H.A. Sober, editor. p. C3. The Chemical Rubber Co., Cleveland

Timchenko, A.A., Ptitsyn, O.B., Troitsky, A.V., Denesyuk, A.I. 1978. The structure of phage *T4* lysozyme in solution noticeably differs from its crystalline structure. *FEBS Lett.* **88**:109

Yang, J.T. 1961. The viscosity of macromolecules in relation to molecular conformation. *In:* Advances in Protein Chemistry. C.B. Anfinsen, M.L. Anson, K. Bailey, and J.T. Edsall, editors. p. 323. Academic Press, New York–London